

Mechanism for thermite reactions of aluminum/iron-oxide nanocomposites based on residue analysis

Yi WANG^{1,2}, Xiao-lan SONG³, Wei JIANG¹, Guo-dong DENG¹, Xiao-de GUO¹, Hong-ying LIU¹, Feng-sheng LI¹

1. National Special Superfine Powder Engineering Research Center,
Nanjing University of Science and Technology, Nanjing 210094, China;

2. School of Materials Science and Engineering, North University of China, Taiyuan 030051, China;

3. School of Chemical Engineering and Environment, North University of China, Taiyuan 030051, China

Received 16 October 2012; accepted 3 December 2012

Abstract: Sol-gel method was employed to combine Al and iron-oxide to form nanocomposites (nano-Al/xero-Fe₂O₃ and micro-Al/xero-Fe₂O₃). SEM, EDS and XRD analyses were used to characterize the nanocomposites and the results indicated that nano-Al and micro-Al were compactly wrapped by amorphous iron-oxide nanoparticles (about 20 nm), respectively. The iron-oxide showed the mass ratio of Fe to O as similar as that in Fe₂O₃. Thermal analyses were performed on two nanocomposites, and four simple mixtures (nano-Al+xero-Fe₂O₃, nano-Al+micro-Fe₂O₃, micro-Al+xero-Fe₂O₃, and micro-Al+micro-Fe₂O₃) were also analyzed. There were not apparent distinctions in the reactions of thermites fueled by nano-Al. For thermites fueled by micro-Al, the DSC peak temperatures of micro-Al/Xero-Fe₂O₃ were advanced by 68.1 °C and 76.8 °C compared with micro-Al+xero-Fe₂O₃ and micro-Al+micro-Fe₂O₃, respectively. Four thermites, namely, nano-Al/xero-Fe₂O₃, nano-Al+micro-Fe₂O₃, micro-Al/xero-Fe₂O₃, and micro-Al+micro-Fe₂O₃, were heated from ambient temperature to 1020 °C, during which the products at 660 °C and 1020 °C were collected and analyzed by XRD. Crystals of Fe, FeAl₂O₄, Fe₃O₄, α-Fe₂O₃, Al, γ-Fe₂O₃, Al_{2.667}O₄, FeO and α-Al₂O₃ were indexed in XRD patterns. For each thermite, according to the specific products, the possible equations were given. Based on the principle of the minimum free energy, the most reasonable equations were inferred from the possible reactions.

Key words: Al; nanocomposites; thermite reaction; reaction mechanism

1 Introduction

As a kind of energetic materials, thermites can release enormous heats during the combustion [1–3]. Certainly, thermite reaction is the chemical reaction that was discovered 200 years ago. They served as solder for rail and powders in combustion bomb because the high burning heats can make steel melt easy and burn down the hard targets. It should (or had) be a good proposal to use these little projectiles as impact initiated energetic materials (i.e. the reactive materials) that had become the focus in the studies about thermites [4,5]. This kind of materials will be ignited by impact action and show their excellent energy release characteristics during penetration process [6,7]. However, the energy release is not the dominating effect for target damage; it is only a complementary of penetration in that course. So, reaction performance of the projectiles becomes the most crucial

factor (the poor performance cannot support the further damage to hard targets in such short time course, i.e. penetration course). In this case, seizing the mechanisms for the reactions of thermites consisting of nanoenergetic composites became very important. The known mechanisms can be used to guide the formulation selection and interpret the results of kinetic and thermodynamic studies.

For the reactions based on solid–solid reaction (in particular reactions between metallic particles and metal oxides), the performance is determined by thermal reactivity of fuel(s) and combination state between fuel(s) and oxidizer(s). For the former, two methods were employed to largely promote the thermal reactivity of aluminum, i.e. using nano-Al or Al-based alloy particles (with nanometer structures) as the fuel(s) [8–12]; for the later, fabricating nanocomposite composed of Al and metal-oxide(s) were investigated [13–15]. These researches employed many classic methods that hastened

the reaction performance, in which the DSC data and burning rates served as the criterion to judge whether reactions were promoted or not. In fact, as known, a thermite reaction that illustrated only one heat release course in a DSC trace may consist of many specific chemical reactions. In particular, when the metal element can bond with other elements at different valence states, thermite reaction becomes rather complex. There were many reports about the reaction mechanisms of Al-Fe₂O₃ systems, but the results were different. MEI et al [16] compressed Al and Fe₂O₃ powders into a slice and heated it to different temperatures. The residues were analyzed by XRD and the products of Al, Fe, Fe₂O₃, Al₂O₃, Fe₃O₄, and FeAl₂O₄ were detected. Accordingly, they inferred that the whole reaction comprised two steps: Above 960 °C, the main reaction was Fe₂O₃→2FeO+0.5O₂; at 960–1060 °C, three reactions (i.e. FeO+Al₂O₃→FeAl₂O₄, Fe₂O₃+2Al→Al₂O₃+2Fe, and 9Fe₂O₃+2Al→6Fe₃O₄+Al₂O₃) took place. GOYA and RECHENBERG [17] also investigated the Al-Fe₂O₃ systems. However, they used mechanical milling to intrigue the thermite reaction and the equation (Al+Fe₂O₃→3Fe_{0.67}Al_{0.33}+1.5O₂) was suggested. CUADRODO also milled the Al-Fe₂O₃ and obtained the products of α-Fe, α-Al₂O₃, Fe-Al, and FeAl₂O₄. The result accorded with that of MATTEAZZI and CAER [18] who considered that the FeAl₂O₄ is the intermediate of the thermite reaction. DURAES et al [19] proposed that the producing of FeAl₂O₄ became more thermodynamically preferential when the mass ratio of Fe₂O₃ to Al was beyond the stoichiometric ratio in the theoretical equation (Fe₂O₃+2Al→Al₂O₃+2Fe).

The abovementioned mechanism researches did not suggest an absolute right result because the mechanism was largely affected by internal or external factors such as ignition, formulation, combination, crystal properties of fuel(s) and oxidizers(s). Hence, the relationship between the reaction performance and reaction mechanism was proposed to take the comparison with the results that are obtained under the same condition. In this work, using 1,2-epoxypropane derived sol-gel method, we combined the fuel (metallic Al) and the oxidizer (iron-oxide) as nanocomposites to improve the thermite reactions. Reaction performance of nanocomposites and simple mixtures was studied by thermal analyses. The reaction products were analyzed and the most proper reaction equations were inferred.

2 Experimental

2.1 Fabrication of Al/iron-oxide nanocomposites

Nanometer and micron Al were respectively used to fabricate nano-Al/xero-Fe₂O₃ and micro-Al/xero-Fe₂O₃

nanocomposites, and the two nanocomposites were prepared by the same sol-gel process. Before fabrication, the aluminum particles were immersed in hot ethanol with agitating. Then the Al particles were added into ethanol solution of Fe(NO₃)₃·9H₂O. The suspension was ultrasonic dispersed for several minutes, then 1,2-epoxypropane was introduced to make it gel. After being aged for 3–5 d, the wet gel was dried in vacuum and the xerogel contained Al particles. The xerogel was washed in ethanol at 45 °C and dried to Al/iron-oxide nanocomposites. In sol-gel process, the 1,2-epoxypropane was very important as a proton scavenger to consume H₃O⁺ and make the solution gel. The gelled medium sustained the suspending Al particles and then the coated structure was formed after being dried. The process is sketchily depicted in Fig. 1.

2.2 Sample characterization

The morphology and surface elements of the samples were examined by S-4800 field-emission scanning electron microscope (SEM) coupled with energy dispersive spectroscopy (EDS). The phase of aluminum/iron-oxide nanocomposites and residues were investigated by a Bruker Advance D8 X-ray diffractometer, using Cu K_α radiation at 40 kV and 30 mA. Differential scanning calorimetry of the thermites was performed on a TA Model Q600 differential scanning calorimeter.

3 Results and discussion

3.1 Morphology and structure analyses

The micron morphologies of Al particles before and after coating are shown in Fig. 2. Raw Al particles showed their diameters of 30–90 nm (for nano-Al) and 1–3 μm (for micro-Al). After sol-gel process, both Al particles were densely wrapped by thick layers that were composed of nanoparticles (about 20 nm). The images roughly consisted with the designed results illustrated in Fig. 1. In our previous work, ammonium perchlorate (AP)/Fe₂O₃ nanocomposites were prepared by the method like this. The TEM images also confirmed the nanosize (about 20 nm) of Fe₂O₃ [20]. The EDS spectra of two nanocomposites were manifested in Fig. 3. It shows that the surface of nanocomposite contains Al, Fe, O and C. The mass ratios of Fe to O in nano-Al/iron-oxide and micro-Al/iron-oxide are 45.89%/22.96% and 43.11%/21.28% respectively, which roughly match with the mass ratio of Fe to O in Fe₂O₃. Accordingly, the iron-oxide coated Al was termed xero-Fe₂O₃ in this work. Figure 4 reveals that the iron-oxide coating on surface of Al is amorphous because all four diffraction peaks at 2θ of 38.47°, 44.90°, 65.09°, and 78.22° respectively refer to the (111), (200), (220), and (311) faces of metallic Al.

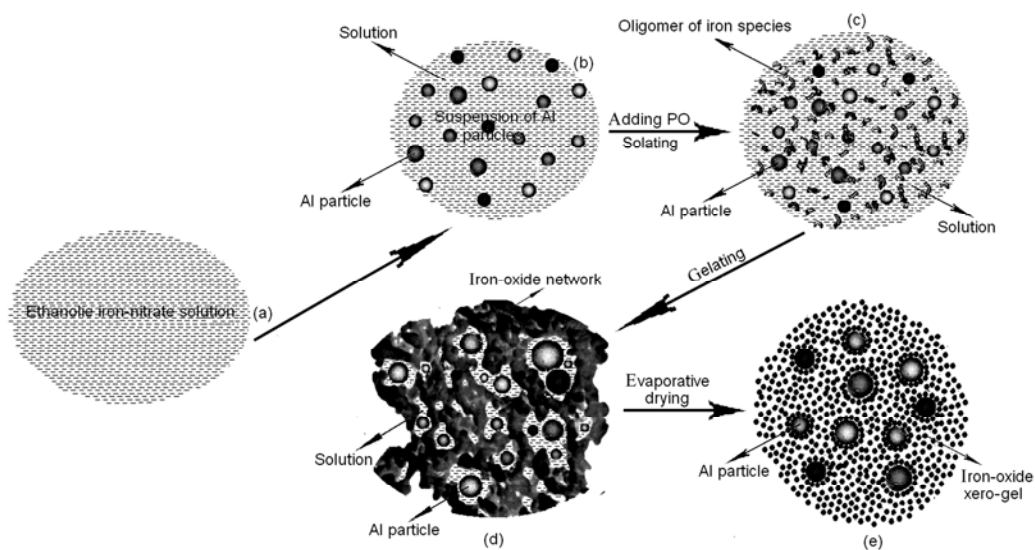


Fig. 1 Sketch for fabrication process of Al/xero-Fe₂O₃ nanocomposites (PO is 1,2-epoxypropane and iron-nitrate is Fe(NO₃)₃·9H₂O)

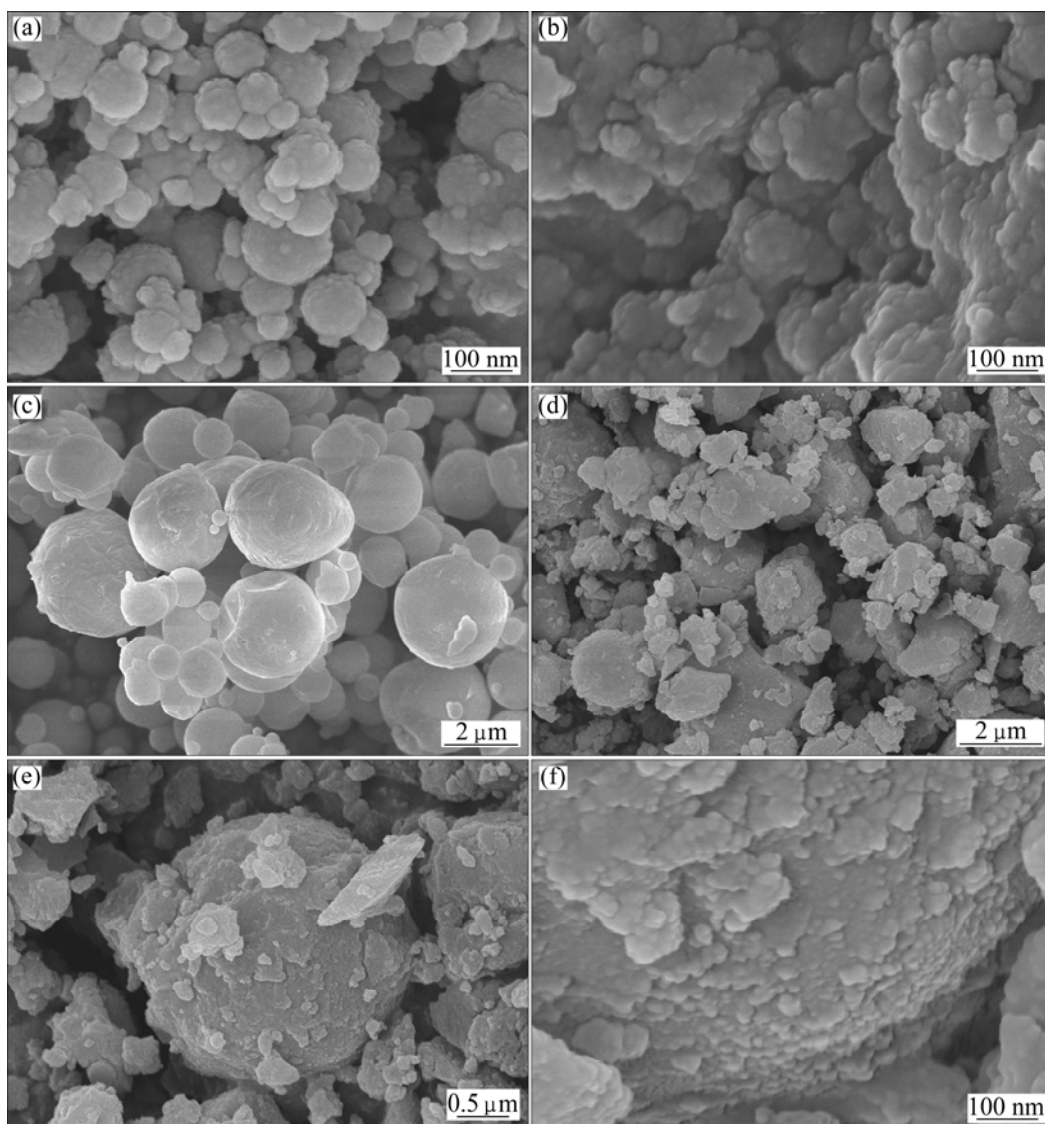


Fig. 2 SEM images of nano-Al (a), nano-Al/xero-Fe₂O₃ (b), micro-Al (c) and micro-Al/xero-Fe₂O₃ (d–f)

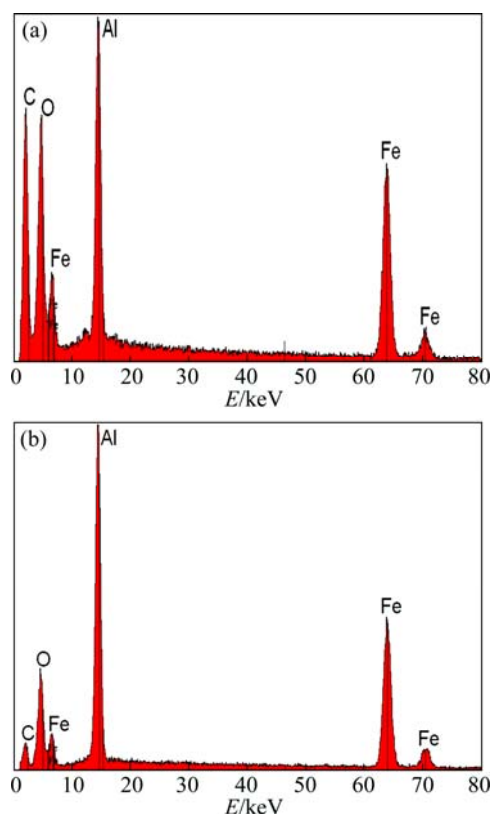


Fig. 3 EDS spectra of nano-Al/xero-Fe₂O₃ (a) and micro-Al/xero-Fe₂O₃ (b)

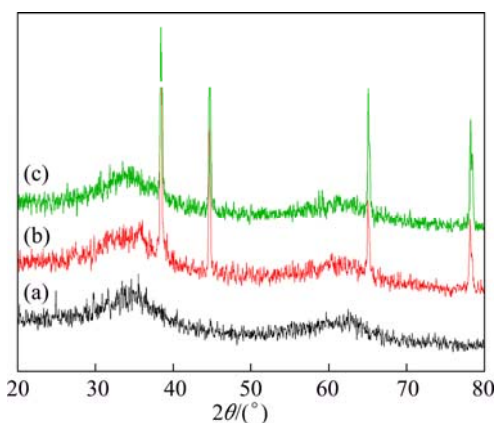


Fig. 4 XRD patterns of xero-Fe₂O₃ (a), nano-Al/xero-Fe₂O₃ (b) and micro-Al/xero-Fe₂O₃ (c)

3.2 Thermal analysis

Thermal analyses for nanocomposites were performed and the results are illustrated in Fig. 5 and Table 1. For comparison, two simple mixtures, Al+xero-Fe₂O₃ and Al+micro-Fe₂O₃ were also analyzed. The xero-Fe₂O₃ was fabricated by the same method as the preparation of nanocomposites. The micro-Fe₂O₃ that was common merchandise (α -Fe₂O₃) was directly used as oxidizer in thermites without any further processing. For nano-Al fueled thermites, there are two exothermic courses and the low-temperature reaction is dominated.

For micro-Al fueled thermites, the exothermic course before melt point of Al is unobvious and thermite reaction occurs at elevated temperature. In fact, in terms of the DSC data in Table 1, nano-Al/xero-Fe₂O₃ did not show distinct superiority versus the simple mixtures. However, for micro-Al fueled thermites, the peak points of micro-Al/xero-Fe₂O₃ compared with simple mixtures were advanced by 68.1 °C and 76.8 °C respectively. This is an obvious promotion for a thermite reaction.

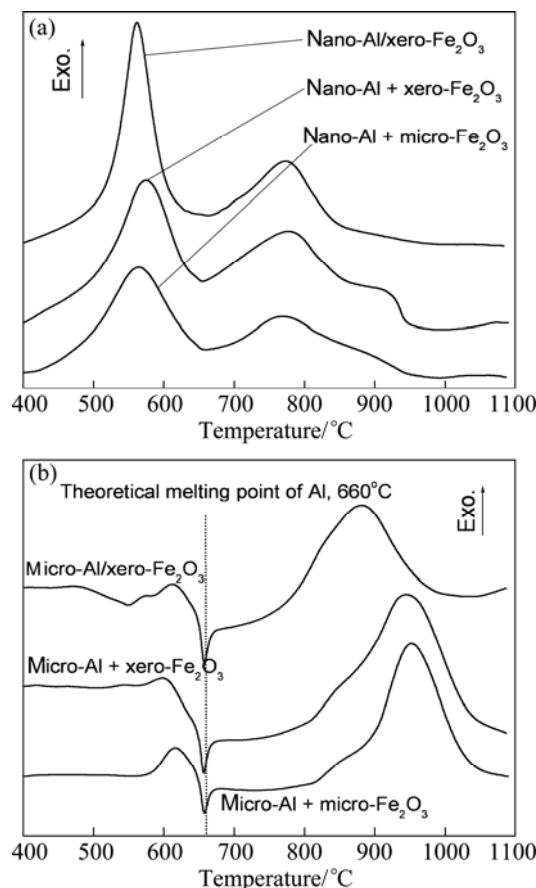


Fig. 5 DSC traces of thermites fueled by nano-Al (a) and micro-Al (b)

3.3 Residues analysis

DSC analyses roughly displayed the heat release profiles of the thermite reaction. The reaction products were identified and the possible reaction equations were inferred. Four samples, nano-Al/xero-Fe₂O₃, nano-Al+micro-Fe₂O₃, micro-Al/xero-Fe₂O₃, and micro-Al+micro-Fe₂O₃ were heated in Ar from ambient temperature to 1020 °C. The residues were collected at 660 °C and 1020 °C respectively and analyzed by XRD. The patterns are presented in Fig. 6, from which nine materials were identified, namely, Fe (08–0722), FeAl₂O₄ (86–2320), Fe₃O₄ (88–0866), α -Fe₂O₃ (84–0308), Al (85–1327), γ -Fe₂O₃ (39–1346), Al_{2.667}O₄ (80–1385), FeO (74–1886) and α -Al₂O₃ (81–2266).

Table 1 DSC data of thermite reactions

Thermite	Combination state	$t_{p-L}/^{\circ}\text{C}$	$t_{p-H}/^{\circ}\text{C}$	$\Delta H_f/(\text{J}\cdot\text{g}^{-1})$	$Q_{\max-L}/(\text{W}\cdot\text{g}^{-1})$	$Q_{\max-H}/(\text{W}\cdot\text{g}^{-1})$
nano-Al/xero- Fe_2O_3	Nanocomposite	561.8	773.2	1648	4.30	1.61
nano-Al+ xero- Fe_2O_3	Simple	571.8	778.4	1505	2.82	1.75
nano-Al+ micro- Fe_2O_3	Simple	564.1	775.3	1397	2.03	1.12
micro-Al/xero- Fe_2O_3	Nanocomposite	—	875.8	889.7	—	2.05
micro-Al+ xero- Fe_2O_3	Simple	—	943.9	955.2	—	2.50
micro-Al + micro- Fe_2O_3	Simple	—	952.6	945.8	—	2.96

t_{p-L} and t_{p-H} represent the peak points of low and high temperature peak, respectively. $Q_{\max-L}$ and $Q_{\max-H}$ represent the maximum heat flows of low and high temperature peak, respectively.

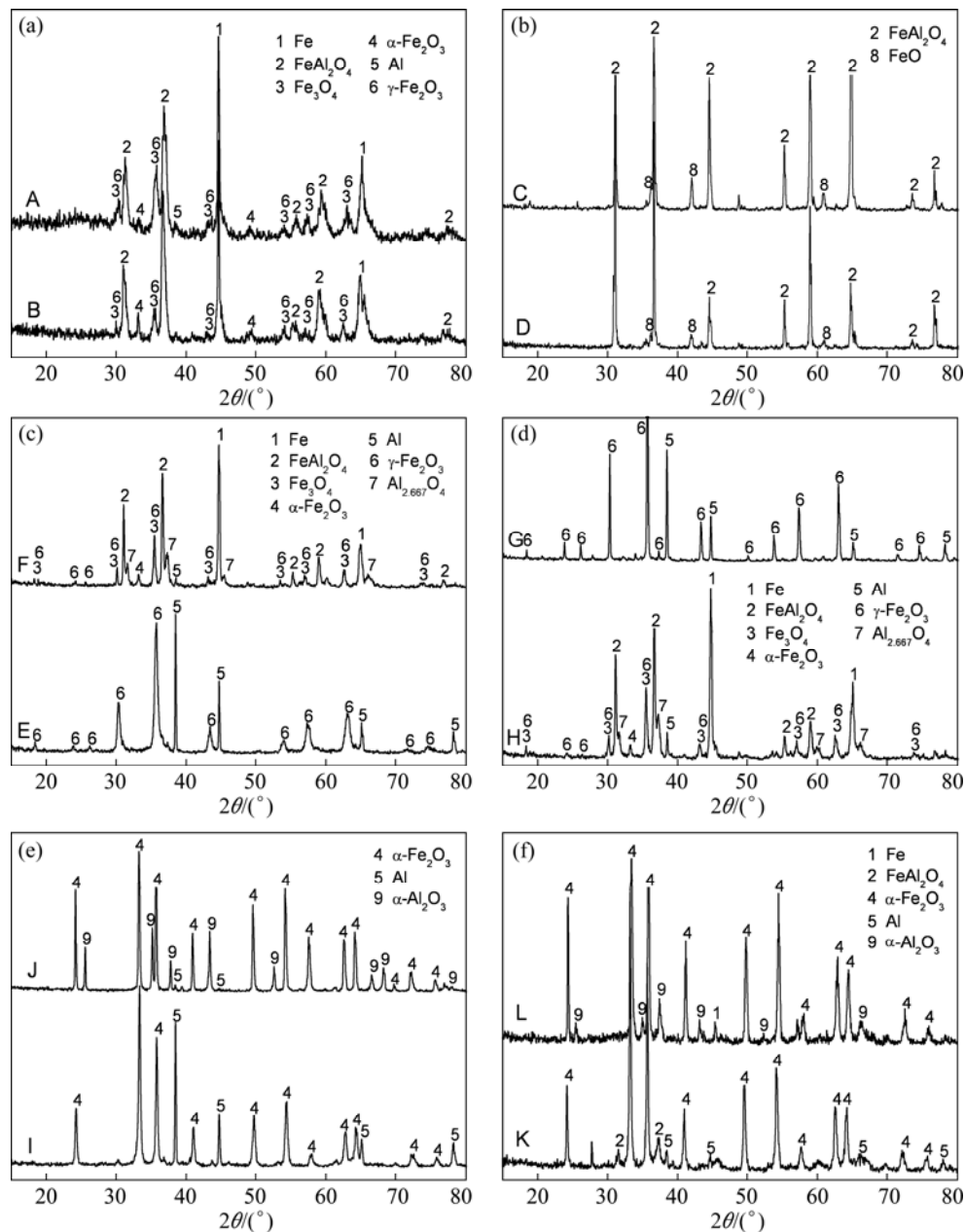


Fig. 6 XRD patterns for residues: (a–d) Samples heated in Ar; (e,f) Samples heated in air (A—Nano-Al/xero- Fe_2O_3 recovered at 660 $^{\circ}\text{C}$; B—Nano-Al/xero- Fe_2O_3 recovered at 1020 $^{\circ}\text{C}$; C—Nano-Al+micro- Fe_2O_3 recovered at 660 $^{\circ}\text{C}$; D—Nano-Al+micro- Fe_2O_3 recovered at 1020 $^{\circ}\text{C}$; E—Micro-Al/xero- Fe_2O_3 recovered at 660 $^{\circ}\text{C}$; F—Micro-Al/xero- Fe_2O_3 recovered at 1020 $^{\circ}\text{C}$; G—Residue of micro-Al/xero- Fe_2O_3 recovered at 660 $^{\circ}\text{C}$; H—Micro-Al+ micro- Fe_2O_3 recovered at 1020 $^{\circ}\text{C}$; I—Micro-Al+micro- Fe_2O_3 recovered at 660 $^{\circ}\text{C}$; J—Residue of micro-Al/xero- Fe_2O_3 recovered at 1020 $^{\circ}\text{C}$; K—Residue of nano-Al/xero- Fe_2O_3 recovered at 660 $^{\circ}\text{C}$; L—Residue of nano-Al/xero- Fe_2O_3 recovered at 1020 $^{\circ}\text{C}$)

In fabrication of nanocomposites, the mass ratio of Al to Fe to O is accordant with the stoichiometric ratio of the equation ($2\text{Al}+\text{Fe}_2\text{O}_3\rightarrow\text{Al}_2\text{O}_3+2\text{Fe}+3.99\text{ kJ/g}$). In comparison with the multi-products detected from the residues, this equation can only be referred to a theoretical reaction. Based on the nine products, possible reactions are suggested and listed in Table 2. In order to

infer the most proper reactions, the plots of ΔG_r vs temperature (for almost all the possible reaction in Table 2) were calculated and presented in Fig. 7. The reaction that is thermodynamically preferential can be inferred by comprehensive analysis on products, possible reactions, and values of ΔG_r .

For nano-Al/xero- Fe_2O_3 , the possible reactions (at

Table 2 Possible reactions resulted from detected products

Equation No.	Possible reaction	Equation No.	Possible reaction
(1)	$\text{xero-Fe}_2\text{O}_3 \rightarrow \gamma\text{-Fe}_2\text{O}_3$	(10)	$1.5\text{FeAl}_2\text{O}_4+\text{Al}\rightarrow 1.5\text{Fe}+2\text{Al}_2\text{O}_3$
(2)	$1.333\gamma\text{-Fe}_2\text{O}_3+2\text{Al}\rightarrow\text{FeAl}_2\text{O}_4+1.667\text{Fe}$	(11)	$2\alpha\text{-Fe}_2\text{O}_3\rightarrow 4\text{FeO}+\text{O}_2$
(3)	$6\gamma\text{-Fe}_2\text{O}_3\rightarrow 4\text{Fe}_3\text{O}_4+\text{O}_2$	(12)	$3\alpha\text{-Fe}_2\text{O}_3+2\text{Al}\rightarrow\text{FeAl}_2\text{O}_4+5\text{FeO}$
(4)	$9\gamma\text{-Fe}_2\text{O}_3+2\text{Al}\rightarrow 6\text{Fe}_3\text{O}_4+\text{Al}_2\text{O}_3$	(13)	$\gamma\text{-Fe}_2\text{O}_3\rightarrow\alpha\text{-Fe}_2\text{O}_3$
(5)	$\gamma\text{-Fe}_2\text{O}_3+2\text{Al}\rightarrow 2\text{Fe}+\text{Al}_2\text{O}_3$	(14)	$\alpha\text{-Fe}_2\text{O}_3\rightarrow\gamma\text{-Fe}_2\text{O}_3$
(6)	$8\gamma\text{-Fe}_2\text{O}_3+2\text{Al}\rightarrow 5\text{Fe}_3\text{O}_4+\text{FeAl}_2\text{O}_4$	(15)	$\alpha\text{-Fe}_2\text{O}_3+2\text{Al}\rightarrow 2\text{Fe}+\alpha\text{-Al}_2\text{O}_3$
(7)	$1.5\gamma\text{-Fe}_2\text{O}_3+2.5\text{Al}_2\text{O}_3+\text{Al}\rightarrow 3\text{FeAl}_2\text{O}_4$	(16)	$2\text{Fe}+1.5\text{O}_2\rightarrow\alpha\text{-Fe}_2\text{O}_3$
(8)	$\text{Fe}_3\text{O}_4+2\text{Al}\rightarrow 2\text{Fe}+\text{FeAl}_2\text{O}_4$	(17)	$1.333\alpha\text{-Fe}_2\text{O}_3+2\text{Al}\rightarrow\text{FeAl}_2\text{O}_4+1.667\text{Fe}$
(9)	$1.5\text{Fe}_3\text{O}_4+4\text{Al}_2\text{O}_3+\text{Al}\rightarrow 4.5\text{FeAl}_2\text{O}_4$	(18)	$4\text{FeAl}_2\text{O}_4+\text{O}_2\rightarrow 2\alpha\text{-Fe}_2\text{O}_3+4\alpha\text{-Al}_2\text{O}_3$

Table 3 Detected products, possible reaction and inferred reactions for different thermites

Thermite	Atmosphere	Temperature/ $^{\circ}\text{C}$	Detected product	Possible reaction	Inferred reaction
nano-Al/ xero- Fe_2O_3	Ar	660	Fe, FeAl_2O_4 , $\gamma\text{-Fe}_2\text{O}_3$, Fe_3O_4	Eqs. (1)–(10)	Eq. (1), Eq. (6), Eq. (8)
	Ar	1020	Fe, FeAl_2O_4 , $\gamma\text{-Fe}_2\text{O}_3$, Fe_3O_4	–	–
nano-Al+ micro- Fe_2O_3	Ar	660	FeAl_2O_4 , FeO	Eq. (11), Eq. (12)	Eq. (12)
	Ar	1020	FeAl_2O_4 , FeO	–	–
micro-Al/ xero- Fe_2O_3	Ar	660	$\gamma\text{-Fe}_2\text{O}_3$, Al	Eq. (1)	Eq. (1)
	Ar	1020	Fe, FeAl_2O_4 , Fe_3O_4 , $\gamma\text{-Fe}_2\text{O}_3$, $\text{Al}_{2.667}\text{O}_4$	Eqs. (2)–(10)	Eq. (4), Eq. (6), Eq. (8)
micro-Al + micro- Fe_2O_3	Ar	660	$\alpha\text{-Fe}_2\text{O}_3$, Al	–	–
	Ar	1020	Fe, FeAl_2O_4 , Fe_3O_4 , $\gamma\text{-Fe}_2\text{O}_3$, $\alpha\text{-Fe}_2\text{O}_3$, $\text{Al}_{2.667}\text{O}_4$, Al	Eqs. (2)–(10), Eq. (18)	Eq. (4), Eq. (6), Eq. (8), Eq. (18)
micro-Al/ xero- Fe_2O_3	Air	660	$\gamma\text{-Fe}_2\text{O}_3$, Al	Eq. (1)	Eq. (1)
	Air	1020	$\alpha\text{-Fe}_2\text{O}_3$, $\alpha\text{-Al}_2\text{O}_3$	Eqs. (15)–(18)	Eq. (15), Eq. (16)
nano-Al/ xero- Fe_2O_3	Air	660	$\alpha\text{-Fe}_2\text{O}_3$, FeAl_2O_4 , Al	Eqs. (1)–(8), Eqs. (13)–(17)	Eq. (1), Eq. (13), Eq. (16), Eq. (17)
	Air	1020	$\alpha\text{-Fe}_2\text{O}_3$, $\alpha\text{-Al}_2\text{O}_3$, Fe	Eq. (10), Eq. (16), Eq. (18)	Eq. (10), Eq. (18)

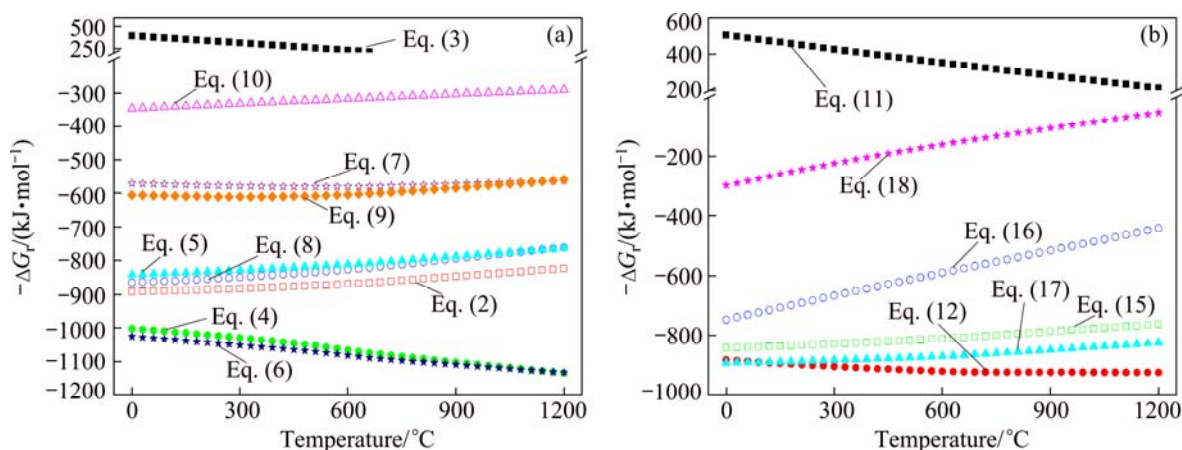


Fig. 7 Plots of ΔG_r vs temperature of possible reactions shown in Table 2

660 °C) involve Eqs. (1)–(10). Firstly, the crystallization of xero-Fe₂O₃ is affirmed by detection of γ -Fe₂O₃. Subsequently, the possible reactions between γ -Fe₂O₃ and metallic Al were summed as Eqs. (4)–(6). Based on the lowest value of ΔG_r , Eq. (6) is the most possible reaction. Fe₃O₄ and FeAl₂O₄ that are the products of Eq. (6) would sequentially react with Al to produce Fe. Accordingly, the possible reactions are Eq. (8) (Fe₃O₄ reacted with Al) and Eq. (10) (FeAl₂O₄ reacted with Al). The quite low ΔG_r determined that Eq. (8) is more suitable than Eq. (10). Hence, the inferred reactions (for heating nano-Al/xero-Fe₂O₃ from ambient temperature to 660 °C) are Eq. (1), Eq. (6), and Eq. (8). In addition, it is proposed that the dominating reactions almost cease at 660 °C because the detected products at 1020 °C are as the same as those at 660 °C. For the nano-Al + micro-Al simple mixture, the possible reactions are Eq. (11) and Eq. (12). Equation (12) is more proper due to the very lower ΔG_r . The products at 1020 °C also do not differ from those at 660 °C.

For micro-Al/xero-Fe₂O₃, no obvious reaction occurred at 660 °C except the crystallization of xero-Fe₂O₃ (Eq. (1)). At elevated temperatures, γ -Fe₂O₃ reacted with available Al and the possible reactions are Eqs. (2)–(10). The method about how the most proper equation was derived is as similar as that of nano-Al/xero-Fe₂O₃. Therefore, the inferred reactions are Eqs. (4), (6), and (8). Al_{2.667}O₄ is almost equivalent to Al₂O₃. This can be ascribed to an incomplete crystallization process of alumina [19]. The mass ratio of Al to O of Al_{2.667}O₄ very approached to that of Al₂O₃. For micro-Al+micro-Fe₂O₃, there were no obvious reactions took place at 660 °C. When the temperature was elevated to 1020 °C, the fuel and the oxidizer reacted and the inferred reactions were Eqs. (4), (6), (8), and (18). Metallic Al was detected in the products, which means lower efficiency for oxidation of micro-Al. As an extra investigation, two nanocomposites, micro-Al/xero-Fe₂O₃ and nano-Al/xero-Fe₂O₃, were also heated in air atmosphere and the products were probed by XRD analysis (see Fig. 6). For micro-Al/xero-Fe₂O₃, the only reaction that xero-Fe₂O₃ crystallized to γ -Fe₂O₃ was founded. The products at 1020 °C suggested the possible reactions of Eqs. (15)–(18). Although the ΔG_r of Eq. (17) is lower than that of Eq. (15), Eq. (15) is more possible than Eq. (17) because the reaction that FeAl₂O₄ was oxidized to α -Fe₂O₃ and α -Al₂O₃ by oxygen (Eq. (18)) is difficult to occur (for its too large ΔG_r); therefore, the inferred reactions are Eqs. (15) and (16); the produced metallic Fe was oxidized by oxygen. For nano-Al/xero-Fe₂O₃, the main reactions occurred before 660 °C and the possible reactions were Eqs. (1)–(8) and Eqs. (13)–(17).

Based on the principle of the minimum free energy, the reactions of Eqs. (1), (2), (14), and (16) were inferred likewise. As heating continued, the produced FeAl₂O₄ reacted with Al and O₂ respectively, namely, Eq. (10) and Eq. (18) were inferred. In addition, the amorphous xero-Fe₂O₃ would transform into two kinds of crystal iron-oxides if the heating processes were conducted under dissimilar atmosphere. In Ar, γ -Fe₂O₃ was obtained; in air, α -Fe₂O₃ was produced.

4 Conclusions

1) Two nanocomposites, nano-Al/xero-Fe₂O₃ and micro-Al/xero-Fe₂O₃, were prepared by a sol–gel process derived by 1,2-epoxypropane. From SEM and XRD analyses, it is observed that amorphous iron-oxides with particle size about 20 nm were densely coated on the surface of nano-Al and micro-Al, respectively. EDS analysis indicated that the iron-oxide had the mass ratio of Fe to O consistent with that in crystal α -Fe₂O₃. Performance of the nanocomposites was investigated by DSC analyses. For comparing, extra thermal analyses were also conducted on four simple mixtures, nano-Al+xero-Fe₂O₃, nano-Al+micro-Fe₂O₃, micro-Al+xero-Fe₂O₃, and micro-Al+micro-Fe₂O₃. The results showed that for thermites fueled by nano-Al, the reaction performance did not present obvious distinction. However, for thermite reactions that used micro-Al as the reducing agent, the DSC peak temperatures of nanocomposite micro-Al/xero-Fe₂O₃ was advanced by 68.1 °C and 76.8 °C respectively compared with simple mixtures. This reduction is referred to a distinct promotion of thermite reaction.

2) Four thermites, nano-Al/xero-Fe₂O₃, nano-Al+micro-Fe₂O₃, micro-Al/xero-Fe₂O₃, and micro-Al+micro-Fe₂O₃, were heated from ambient temperature to 1020 °C, during which the products at 660 °C and 1020 °C were collected and analyzed. According to the products detected from XRD patterns, there are some possible reactions. Based on the principle of the minimum free energy, the most tenable reactions were inferred from the possible reactions. Products Fe, FeAl₂O₄, Fe₃O₄, α -Fe₂O₃, Al, γ -Fe₂O₃, Al_{2.667}O₄, FeO, and α -Al₂O₃ were detected. These products imply that the reaction $2\text{Al}+\text{Fe}_2\text{O}_3\rightarrow\text{Al}_2\text{O}_3+2\text{Fe}$ is only a theoretical equation; in fact, practical reactions would be far more complex.

References

- [1] ZHU He-gou, WU Shen-qing, WANG Hen-zhi. Thermodynamics analysis of Al₂O₃, TiB₂/Al composites fabricated by exothermic dispersion method [J]. The Chinese Journal of Nonferrous Metals, 2001, 12(3): 382–385. (in Chinese)

- [2] KIM D K, BAE J H, KANG M K. Analysis on thermite reactions of CuO nanowires and nanopowders coated with Al [J]. *Current Applied Physics*, 2011, 11(4): 1067–1070.
- [3] BAZYN T, LYNCH P, KRIER H. Combustion measurements of fuel-rich aluminum and molybdenum oxide nano-composite mixtures [J]. *Propellants, Explosives, Pyrotechnics*, 2010, 35(2): 93–99.
- [4] HUNT E M, MALCOLM S, PANTOYA M L. Impact ignition of nano and micron composite energetic materials [J]. *International Journal of Impact Engineering*, 2009, 36: 842–846.
- [5] DOLGOBORODOV A Y, STRELETSKII A N, MAKHOV M N. Explosive compositions based on the mechanoactivated metal-oxidizer mixtures [J]. *Russian Journal of Physical Chemistry B: Focus on Physics*, 2008, 51(6): 606–611.
- [6] DOLGOBORODOV A Y, MAKHOV M N, KOLBANEV I V. Detonation in an aluminum-Teflon mixture [J]. *JETP Letters*, 2006, 81(7): 311–314.
- [7] BOUMA R H B, MEUKEN D, VERBEEK R. Shear initiation of Al/MoO₃-based reactive materials [J]. *Propellants, Explosives, Pyrotechnics*, 2007, 32(6): 447–453.
- [8] SHOSHIN Y L, MUDRYY R S, DREIZIN E L. Preparation and characterization of energetic Al–Mg mechanical alloy powders [J]. *Combustion and Flame*, 2002, 128: 259–269.
- [9] SHOSHIN Y L, TRUNOV M A, ZHU Xiao-ying. Ignition of aluminum-rich Al–Ti mechanical alloys in air [J]. *Combustion and Flame*, 2006, 144: 688–697.
- [10] SHOSHIN Y L, DREIZIN E L. Particle combustion rates for mechanically alloyed Al–Ti and aluminum powders burning in air [J]. *Combustion and Flame*, 2006, 145: 714–722.
- [11] WANG Yi, JIANG Wei, ZHANG Xian-feng. Energy release characteristics of impact-initiated energetic aluminum–magnesium mechanical alloy particles with nanometer-scale structure [J]. *Thermochimica Acta*, 2011, 512: 233–239.
- [12] WANG Yi, JIANG Wei, LIANG Li-xin. Thermal reactivity of nanostructure Al_{0.8}Mg_{0.2} alloy powder used in thermites [J]. *Rare Metal Materials and Engineering*, 2012, 41(1): 9–13.
- [13] UMBRAJKAR S M, SCHOENITZ M, DREIZIN E L. Exothermic reaction in Al–CuO nanocomposites [J]. *Thermochimica Acta*, 2006, 451: 34–43.
- [14] TILLOTSON T M, GASH A E, SIMPSON R L. Nanostructured energetic materials using sol–gel methodologies [J]. *Journal of Non-Crystalline Solids*, 2001, 285: 338–345.
- [15] SCHOENITZ M, WARD T S, DREIZIN E L. Fully dense nano-composite energetic powders prepared by arrested reactive milling [J]. *Proceedings of the Combustion Institute*, 2005, 30: 2071–2078.
- [16] MEI J, HALLDEARN R D, XIAO P. Mechanisms of the aluminium-iron oxide thermite reaction [J]. *Scripta Materialia*, 1999, 41(5): 541–548.
- [17] GOYA G F, RECHENBERG H R. Mechanochemical synthesis of intermetallic Fe_{100-x}Al_x obtained by reduction of Al/Fe₂O₃ composite [J]. *Journal of Physics: Condensed Matter*, 2000, 12: 10579–10590.
- [18] MATTEAZZI P, CAER G L. Synthesis of nanocrystalline aluminum-metal composites by room temperature ball-milling of metal oxides and aluminum [J]. *Journal of the American Ceramic Society*, 1992, 75: 2749–2755.
- [19] DURAES L, COSTA B F O, SANTOS R. Fe₂O₃/aluminum thermite reaction intermediate and final products characterization [J]. *Materials Science and Engineering A*, 2007, 456: 199–210.
- [20] SONG X L, LI F S, ZHANG J L. Preparation, mechanical sensitivity and thermal decomposition of AP/Fe₂O₃ nanocomposite [J]. *Journal of Solid Rocket Technology*, 2009, 32(3): 306–309.

基于产物分析的铝/铁氧化物纳米复合材料的铝热反应机理

王毅^{1,2}, 宋小兰³, 姜炜¹, 邓国栋¹, 郭效德¹, 刘宏英¹, 李凤生¹

1. 南京理工大学 国家特种超细粉体工程技术研究中心, 南京 210094;

2. 中北大学 材料科学与工程学院, 太原 030051; 3. 中北大学 化工与环境学院, 太原 030051

摘要: 采用溶胶–凝胶法分别对纳米 Al 和微米 Al 进行表面包覆, 制备 nano-Al/xero-Fe₂O₃ 和 micro-Al/xero-Fe₂O₃ 2 种复合材料, 并对它们的微观结构和物相进行表征。结果表明, 纳米 Al 和微米 Al 表面均被约 20 nm 的无定形纳米粒子致密包覆; 包覆物中的铁氧比与 Fe₂O₃ 中的铁氧比大致相当。对 2 种纳米复合材料以及 4 种相对应的简单混合物(nano-Al+xero-Fe₂O₃、nano-Al+micro-Fe₂O₃、micro-Al+xero-Fe₂O₃ 和 micro-Al+micro-Fe₂O₃) 分别进行 DSC 分析。对于采用纳米 Al 作燃料的铝热剂, nano-Al/xero-Fe₂O₃、nano-Al+xero-Fe₂O₃ 和 nano-Al+micro-Fe₂O₃ 三者的热谱图没有明显差别; 对于采用微米 Al 作燃料的铝热剂, micro-Al/xero-Fe₂O₃ 的反应峰温度较 micro-Al+xero-Fe₂O₃ 和 micro-Al+micro-Fe₂O₃ 的分别提高了 68.1 °C 和 76.8 °C。另外, 将 4 种铝热剂(nano-Al/xero-Fe₂O₃、nano-Al+micro-Fe₂O₃、micro-Al/xero-Fe₂O₃ 和 micro-Al+micro-Fe₂O₃) 同时从室温加热至 1020 °C, 对 660 °C 和 1020 °C 时的产物进行 XRD 分析。从图谱中共检测出 Fe、FeAl₂O₄、Fe₃O₄、 α -Fe₂O₃、Al、 γ -Fe₂O₃、Al_{2.667}O₄、FeO 和 α -Al₂O₃ 共 9 种晶体物质。据此推测了可能的反应方程, 并以最小自由能原则推出了每种样品最可能的反应过程。

关键词: Al; 纳米复合物; 铝热反应; 反应机理

(Edited by Xiang-qun LI)